1-9-2006

Application of an HP-Adaptive Finite Element Method for Thermal Flow Problems

Xiuling Wang
Nevada Center for Advanced Computational Methods

Darrell Pepper
University of Nevada, Las Vegas, darrell.pepper@unlv.edu

Application of an *hp*-adaptive Finite Element Method for Thermal Flow Problems

Xiuling Wang[*] and Darrell W. Pepper[†]

University of Nevada Las Vegas, 4505 Maryland Parkway, Las Vegas, NV 89154-4027

Numerical results are presented for a set of convective thermal flow problems using an *hp*-adaptive finite element technique. The *hp*-adaptive model is based on mesh refinement and spectral order incensement to produce enhanced accuracy while attempting to minimize computational requirements. An *a-posteriori error* estimator based on the L_2 norm is employed to guide the adaptation procedure. Example test cases consisting of natural convection in a differentially heated enclosure, flow with forced convection heat transfer over a backward facing step and natural convection within an enclosed partition are presented. Numerical results are compared with published data in the literature.

Nomenclature

A	Advection matrix
B	Body force
F_v	Load vector for velocity
F_T	Load vector for temperature
h_e	Characteristic element length
h	Element size
t	Time
T	Temperature
k_h	Diffusion coefficient
K_v	Diffusion matrix for velocity
K_T	Diffusion matrix for temperature
M	Mass matrix
N_i	Shape function
p	Shape function order
P	Pressure
P_r	Prandtl number
P_e	Peclet number
R_e	Reynolds number
R_a	Rayleigh number
V	Velocity vector
α	Petrov-Galerkin weighting factor
γ	Petrov-Galerkin stability parameter
ρ	Density
L	Linear orthogonal projection operator
∇	Divergence operator

[*] Postdoctoral Fellow, Nevada Center for Advanced Computational Methods (NCACM), AIAA Member
[†] Professor of Mechanical Engineering and Director, NCACM; AIAA Associate Fellow

I.   Introduction

The finite element method (FEM) is one of the most popular numerical tools for solving thermal flow problems, due to its ability to easily deal with irregular geometries, accuracy, and use of general-purpose algorithms. Adaptive FEM is especially powerful as it can provide significantly enhanced accuracy with less computational cost than using uniform refined and enriched meshes.

There are four main categories of adaptation: (1) *h*-adaptation, where the element sizes vary while the order of the shape functions are constant; (2) *p*-adaptation, where the element sizes are constant while the order of the shape functions increase to meet desired accuracy requirements; (3) *r*-adaptation, where the nodes are redistributed in an existing mesh in the process of adaptation; (4) *hp*-adaptation, which is the combination of both *h*- and *p*-adaptation. *hp*-adaptive schemes are among the best mesh-based schemes with the potential payoff of obtaining exponential convergence rates [1] [2]. However, limited applications of *hp*-adaptive techniques for solving fluid flow problems are seen in the literature and even less for solving fluid flow with heat transfer [3] - [6].

In this study, an *hp*-adaptive FEM is employed to solve incompressible flows with heat transfer effects. The basic methodology and adaptive strategy are presented for the numerical model. The numerical model is validated using benchmark problems for flow with forced convective heat transfer over a backward facing step and natural convection within a differentially heated enclosure. Results are compared with published data. Natural convection within a partitioned enclosure is also examined.

II.   *hp*-Adaptive Finite Element Model

The nondimensional form of the governing equations for convective thermal flow can be written as:

Continuity equation:

$$\nabla \bullet V = 0 \tag{1}$$

Momentum equation:

$$\frac{\partial V}{\partial t} + V \bullet \nabla V = -\nabla p + C_{visc}\nabla^2 V + C_{grav}T \tag{2}$$

Energy equation:

$$\frac{\partial T}{\partial t} + V \bullet \nabla T = C_{viscT}\nabla^2 T \tag{3}$$

For forced and natural convection problems, the corresponding values for C_{visc}, C_{viscT} and C_{grav} are listed in Table 1.

Table 1. C_{visc} C_{viscT} C_{grav} **Values**

Convection	C_{visc}	C_{viscT}	C_{grav}
Forced	**1 / Re**	**1 / Pe**	**0**
Natural	**Pr**	**1**	**Pr Ra**

Applying the Galerkin weighted residual method and replacing the variables V and T with the trial functions

$$V(\mathbf{x}, t) = \sum N_i(\mathbf{x})V_i(t) \tag{4}$$

$$T(\mathbf{x}, t) = \sum N_i(\mathbf{x})T_i(t) \tag{5}$$

the matrix equivalent forms for the integral expressions can be obtained:

$$[M]\{\dot{V}\} + ([K] + [A(V)])\{V\} = \{F_V\} \tag{6}$$

$$[M]\{\dot{T}\} + ([K_T] + [A(V)])\{T\} = \{F_T\} \tag{7}$$

2
American Institute of Aeronautics and Astronautics

The governing equations are solved using a projection algorithm. Detailed descriptions regarding projection algorithms are discussed in Chorin et al [7]. The matrix coefficients in the finite element formulations are defined as (summation convention is employed):

$$[M] = \int_\Omega N_i N_j d\Omega \tag{8}$$

$$A(V) = \int_\Omega N_i (N_k V_k) \frac{\partial N_j}{\partial x_j} d\Omega \tag{9}$$

$$[K_V] = \int_\Omega C_{visc} \frac{\partial N_i \partial N_j}{\partial x_i \partial x_j} d\Omega \tag{10}$$

$$[K_T] = \int_\Omega C_{viscT} \frac{\partial N_i \partial N_j}{\partial x_i \partial x_j} d\Omega \tag{11}$$

$$\{F_v\} = \int_\Omega N_i f(x_i) d\Omega + \int_\Gamma C_{visc} N_i n_i \frac{\partial V_j}{\partial x_j} d\Gamma \tag{12}$$

$$\{F_T\} = \int_\Omega N_i Q d\Omega + \int_\Gamma N_i q d\Gamma \tag{13}$$

A Petrov-Galerkin scheme is used to weight the advection terms in the governing equations. The altered weighting function skews the interpolation function in the upwind direction so that dispersion and added diffusion introduced by the standard Galerkin formulation can be minimized. The weighting scheme is defined as

$$W_i = N_i + \frac{\alpha h_e}{2|V|} [V \cdot \nabla N_i] \tag{14}$$

$$\alpha = \coth \frac{\gamma}{2} - \frac{2}{\gamma} \tag{15}$$

where α is Petrov-Galerkin weighting factor, h_e is the characteristic element length and γ is the Petrov-Galerkin stability parameter.

For forced and natural convection problems, the corresponding values for γ are listed in Table 2.

Table 2. γ Values

Convection	γ
Forced	$|V| h_e \, \mathrm{Re} \cdot \mathrm{Pr}$
Natural	$|V| h_e Ra \cdot \mathrm{Pr}$

Mass lumping is used to obtain a fully explicit time scheme. The inverse of the mass matrix becomes:

$$[M]^{-1} = \frac{1}{m_i} \tag{16}$$

The most important rules in adaptive FEM procedures are listed as: (1) 1-Irregular mesh adaptation rules for *h*-adaptation: an element is refined only if its neighbors are at the same or higher level (1-Irregular mesh). This rule guarantees that multiple constraint nodes are avoided; (2) the minimum rule is followed in *p*-adaptation: the order for an edge common for two elements never exceeds the orders of the neighboring middle nodes; (3) the adaptation rules for *h*- and *p*- are combined together in *hp*-adaptation. In addition to these rules, continuity of the global basis functions are also required – this is achieved by employing constraints at the interfaces of elements supporting edge functions of different order.

Various adaptation strategies exist in literature [8] – [11]. The *hp*-adaptive FEM strategy employed in this study follows three steps and guided by an *a posterior error* estimator which is based on the L_2 norm calculation: three consecutive *hp*- adaptive meshes are constructed for solving the system in order to reach a preset target error: an initial coarse mesh, the intermediate *h*-adaptive mesh, and the final *hp*- adaptive mesh obtained by applying *p*-adaptive enrichments on the intermediate mesh. The *p*- adaptation is continued when the problem solution is pre-asymptotic.

III.   Natural Convection in a Squared Enclosure

Many engineering problems of practical interest deal with buoyant flows in enclosures, such as thermal insulation of buildings, heat transfer within attics and roofs, cooling of nuclear reactor cores, etc. Natural convection in a square enclosure has been studied extensively over the past 30 years. In 1983, De Vahl Davis [12] provided accurate benchmark solutions for natural convection in a square enclosure using a finite difference streamfunction/vorticity formulation with an 81 x 81 mesh.

In this study the *hp*-adaptive FEM algorithm is first applied to solve natural convection heat transfer in a differentially heated squared enclosure with Ra = 10000.

Figure 1 shows the problem geometry and boundary conditions. The nondimensional enclosure ($0 \le x \le 1, 0 \le y \le 1$) is heated on one wall, cooled on the other, with the top and bottom walls insulated.
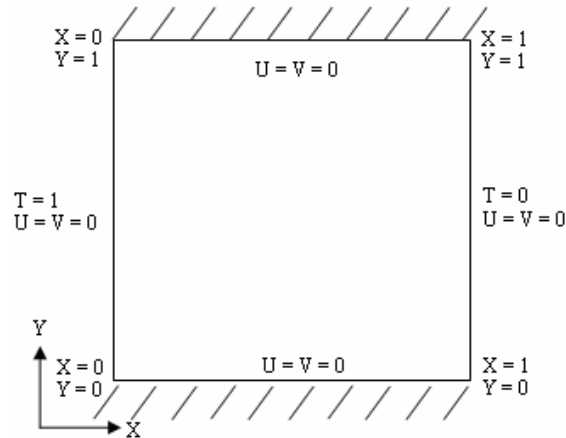

Fig. 1   Geometry and boundary condition for 2-D Natural Convection.

An initial computation is based on a coarse mesh consisting of 20 x 20 bilinear quadrilateral elements. The initial order for the coarse mesh is 1. The final *hp*-adapted mesh is shown in Fig. 2. The total number of elements in the final mesh is 1894 with 5469 DOF. The final mesh is obtained after 3-level *h*- and *p*-adaptation. The mesh is refined and enriched in the boundary layers along the walls.
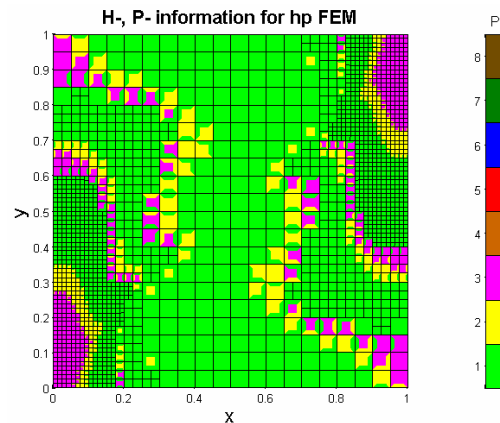

Fig. 2   Final *hp*-adaptive mesh for Ra=10^4

Steady state results are shown in Figs. 3 - 5 for velocity vectors, streamlines and isotherms, respectively. Results compared to de Vahl Davis [12] are listed in Table 3.
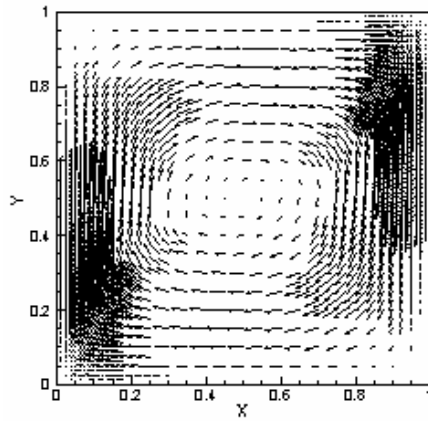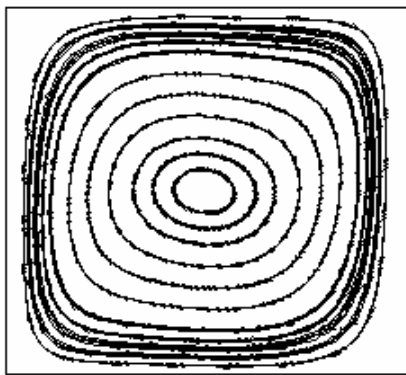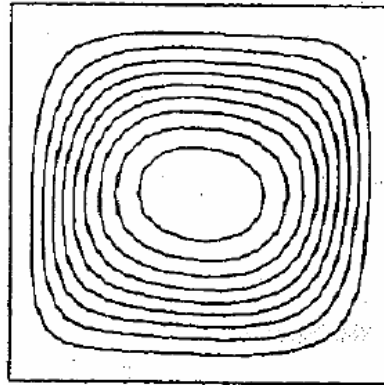
4
American Institute of Aeronautics and Astronautics

Fig. 3   Velocity vectors for Ra=10^4
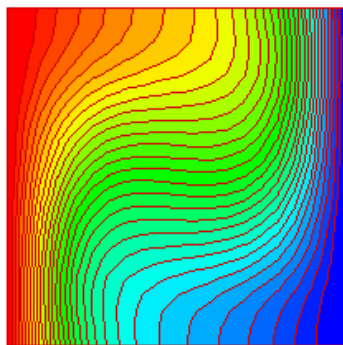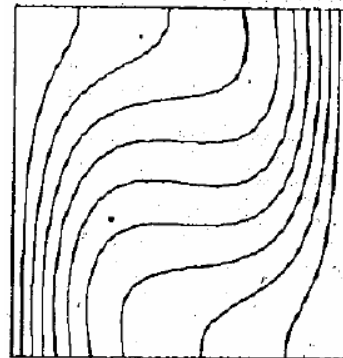

| (a) | (b) |

Fig. 4   Streamlines for Ra=10^4 (a) *hp*-adaptive results (b) benchmark results [12]

| (a) | (b) |

Fig. 5   Isothermals for Ra=10^4 (a) *hp*-adaptive results (b) benchmark results [12]

Table 3. Comparison solutions for 2D natural convection in an enclosure

Case	Pr	Ra	U_{max} (x)	U_{max} (y)	V_{max} (y)	V_{max} (x)
Benchmark [12]	0.7	10^4	16.178	0.823	19.617	0.119
Present results	0.7	10^4	16.180	0.827	19.600	0.120

IV.   Forced Convection in a 2D Backward Facing Step

Two-dimensional flow over a backward facing step is a well known benchmark case which has been studied extensively over many years. The problem is easy to set up with known (expected) results at various Reynolds numbers.

In 1992, Blackwell and Pepper [13] introduced the problem of flow over a backward facing step with heat transfer as a benchmark test problem. Twelve different numerical simulations were presented and the results were compared with the numerical results obtained by Gartling [14] and experimental results from Armaly et al. [15].

In this study, the *hp*-adaptive algorithm is applied to the backward facing step with heat transfer effects. For comparative purposes, Re = 800 and Pr = 0.71. The boundary conditions settings are the same settings as Blackwell and Pepper [13]:

For inlet flow:

$$u(y) = \begin{cases} 0, for 0 \le y \le \dfrac{1}{2} \\ 8y(1-2y), for \dfrac{1}{2} < y \le 1 \end{cases} \tag{17}$$

$$v(y) = 0 \tag{18}$$

$$T(y) = \left[1 - (4y-1)^2\right]\left[1 - \frac{1}{5}(4y-1)^2\right] for \frac{1}{2} < y \le 1 \tag{19}$$

$$\frac{\partial T(y)}{\partial x} = 0 \, for \, 0 \le y < \frac{1}{2} \tag{20}$$

On upper and lower walls:

$$u(y) = v(y) = 0 \tag{21}$$

$$\nabla T \cdot \hat{n} = \frac{32}{5} \tag{22}$$

where $\hat{n}$ is the outward unit vector normal to the domain boundary. For outlet flow,

$$p = 0 \tag{23}$$

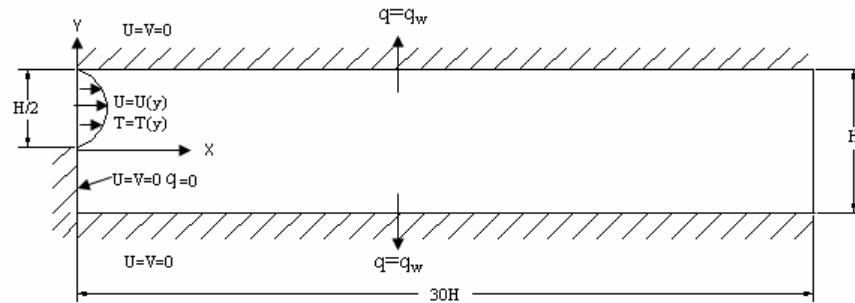The problem configuration and boundary conditions are shown in Fig. 6.

Fig. 6 Problem configuration and boundary conditions

The initial mesh consists of 700 elements and 765 DOFs. The intermediate *h*-adaptive mesh shown in Fig. 7 consists of 1762 elements and 1760 DOFs, which is obtained after a 3-level *h*-adaptation. The final *hp*-adaptive mesh is obtained for up to 3-level *p*- adaptation on the intermediate *h*-adaptive mesh, which is shown in Fig. 8. The final mesh consists of 1762 elements and 3802 DOFs (x:y ratio is 0.25).
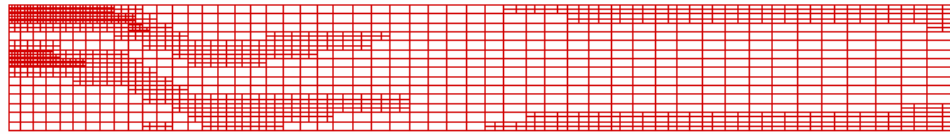
American Institute of Aeronautics and Astronautics

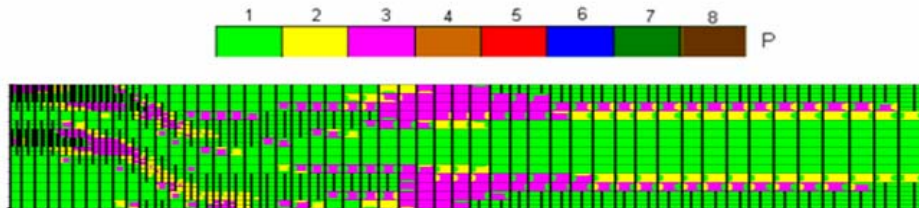**Fig. 7   Intermediate *h*-adaptive mesh**

Fig. 8   Final *hp*-adaptive mesh

Steady state simulation results for streamfunction and temperature are shown in Figs. 9 and 10, respectively.
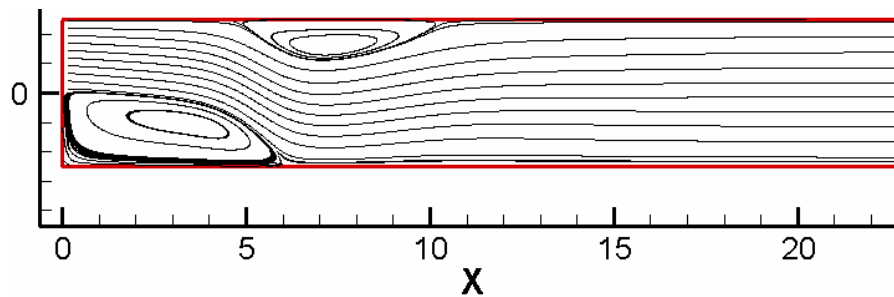

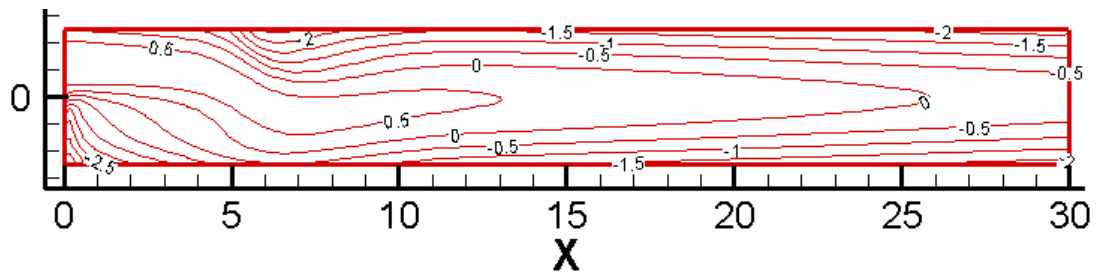**Fig. 9   Streamfunction contours**

Fig. 10 Isotherms

The locations and sizes of the lower wall eddy and upper wall eddy are listed in Tables 4 and 5 and compare closely with results obtained by Gartling [14]. Comparisons of velocity profiles at different cross sessions are made between the *hp*-adaptive results and benchmark data from Gartling [14], which are shown in Fig. 11. Temperature profiles are compared between present *hp*-adaptive results and Emery et al's and Dyne et al's results from [13], which are shown in Fig. 12. Excellent agreement is observed.

Table 4. Comparison of lower wall eddy locations and sizes with the bench mark solution by Gartling [14]

Case	Vortex Center (x, y)	Cell Length (H)
Benchmark [14]	(3.35, -0.2)	6.10
Present result	(3.35, -0.2)	6.00

Table 5. Comparison of upper wall eddy locations and sizes with the bench mark solution by Gartling [14]

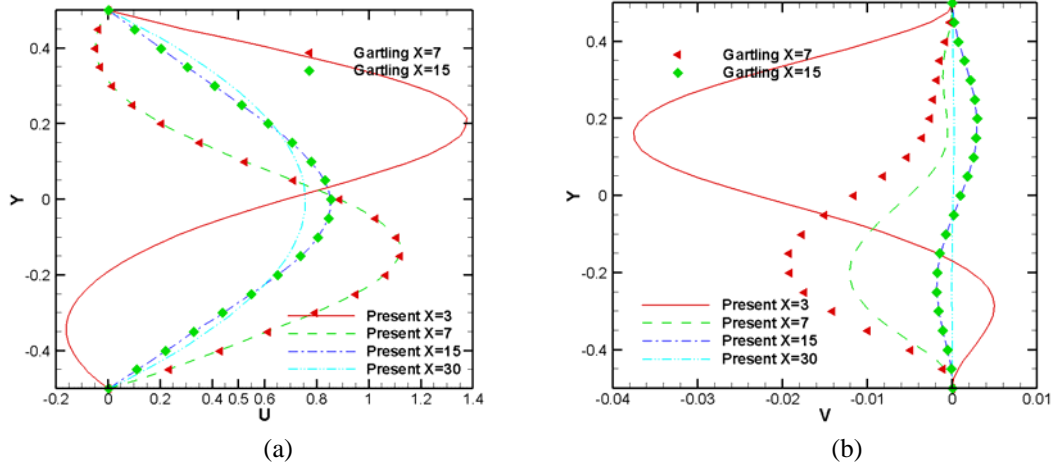| Case	Vortex Center (x, y)	Separation (x, y)	Reattachment (x, y)	Cell Length (H)
Benchmark [14]	(7.40, 0.30)	(4.85, 0.5)	(10.48, 0.5)	5.63
Present result	(7.39, 0.31)	(4.81, 0.5)	(10.45, 0.5)	5.56

(a) (b)

Fig. 11 Comparison of velocity profiles
(a) u profile compared with [14] (b) v profile compared with [14]
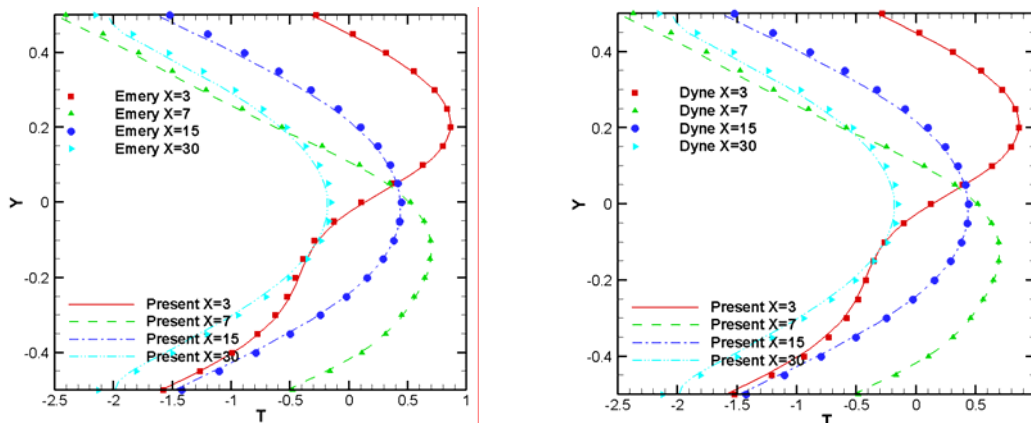

Fig. 12 Comparison of temperature profiles (a) T profile compared with Emery et al.'s results [13] (b) T profile compared with Dyne et al.'s results [13]

V.   Natural Convection in an Enclosed Partition

Natural convection in partially divided enclosures has attracted the attention of both experimental and theoretical researchers in recent years. Practical applications include heat transfer across thermo pane windows, solar collectors, fire spread and energy transfer in rooms and buildings, cooling of nuclear reactors and heat exchanger design [16].

In many situations, a partial obstruction extends from a surface, e.g., a printed circuit or a ceiling beam in a room. Research results show that the heat transfer between two heated side walls is reduced when a partial partition is present.

The partition, along with the top and bottom walls, is insulated. The left and right walls are maintained at hot and cold temperatures, respectively; Ra=10^4. The problem domain is defined as $0 \le x \le 2, 0 \le y \le 1$, as shown in Fig. 13.
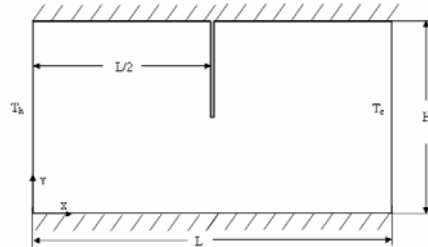

Fig. 13 Partial divided enclosure

The initial coarse mesh consisted of 820 quadrilateral elements with 893 nodes, as shown in Fig. 14. The initial order for the coarse mesh is 1.
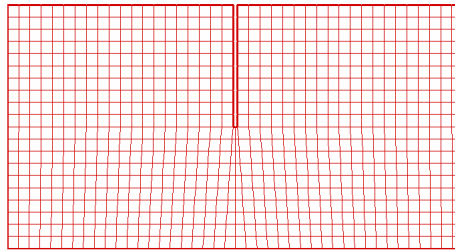

Fig. 14 Initial computational mesh

The final *hp*-adaptive mesh is shown in Fig. 15. The *h*-adaptation preceded over 3 levels while the *p*-adaptation reached 3rd order. The final mesh consists of 3313 elements and 6926 DOF.
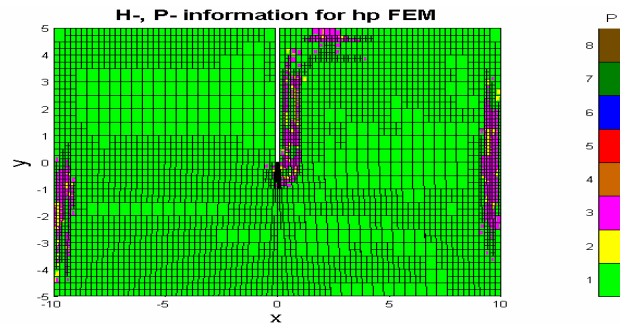

Fig. 15 Final *hp*- adaptive mesh

It can be seen from the final adapted mesh that the mesh is finer in the vertical boundary layers, along with higher order shape functions. This occurs as a result of the flow becoming accelerated around the partition corners and along the vertical walls.

American Institute of Aeronautics and Astronautics

Fig. 16 Error distributions
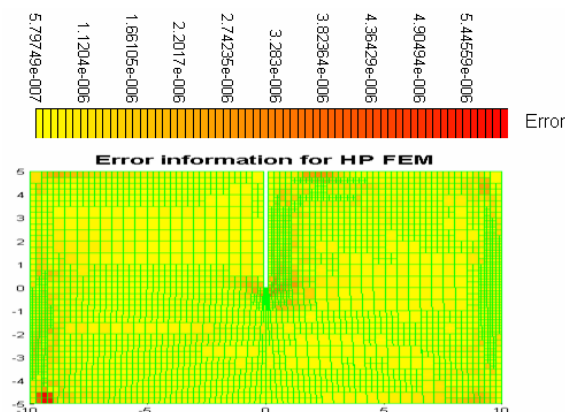
The error distribution shown in Fig. 16 shows those regions of the problem domain where much of the activity is generated with regards to both *h-* and *p*-adaptation, and closely follows the pattern exhibited in Fig. 15.

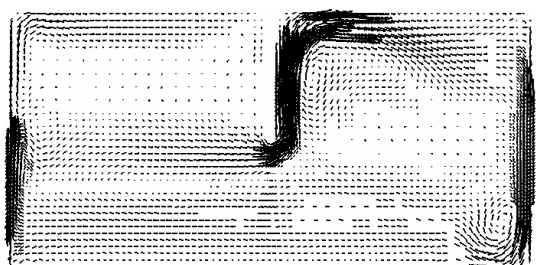Steady state results for velocity vectors and temperature are shown in Figs. 17 and 18, respectively.
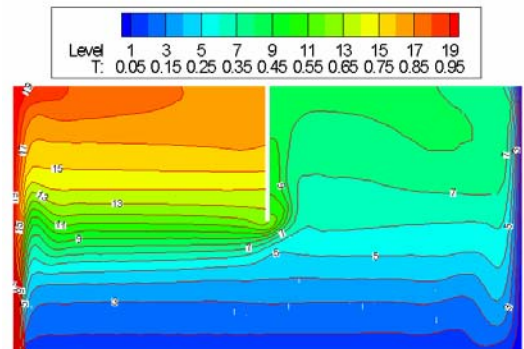

Fig. 17 Velocity vectors

Fig. 18 Temperature contours

VI. Discussion

In order to initially determine the computational efficiency of the adaptive algorithms, the following numerical experiment was conducted: solve for differentially heated natural convection within an enclosure with Ra = 10^5 using a globally uniform *h*- refined and *p*- enriched mesh (uniform refine up to 3-levels and uniform enrichment up to 3rd order) and the *hp*-adaptive algorithm (refined up to 3-levels and enriched to 3rd order). Results show that the globally *h*- refined and *p*- enriched algorithm consumed almost 18X more CPU time (projected) than the *hp*-adaptive algorithm. The employment of the *hp*- adaptive algorithm significantly reduced the computational effort, as shown in Table 6.

Table 6. CPU time comparison between uniform refined/enriched algorithm and *hp*-adaptive algorithm

Compare Cases	# of element		# of DOF		Total CPU Time (sec)	Per DOF CPU time (sec/DOF)	# of iteration
	Initial	Final	Initial	Final			
Uniform *h* (3-level) and *p* (3rd order)	1600	1600	14641	14641	**140884**	9.62	34500
hp-adaptive algorithm(up to 3-level *h*-, 3rd order *p*-)	100	436	121	1385	**7741**	5.59	35519

VII. Conclusion and future work

In this study, an *hp*-adaptive finite element technique has been developed and applied to both forced and natural convection problems. The *hp*-adaptive algorithm utilizes both mesh refinement (*h*) and spectral order incensement (*p*). The numerical method generates very accurate results with less computational effort than globally fine meshes attempting to achieve similar residual error. Thermal problems such as natural convection in a square enclosure, forced convection heat transfer associated with flow downstream of a backward facing step, and natural convection in a partition enclosure are investigated. Results agree well with data in the literature.

References

[1]Guo, B. and Babuska, I., "The *h-p* Version of the Finite Element Method", Parts 1 and 2, *Computational Mechanics*, Vol. 1, pp. 21-21 and pp. 203-220, 1986.

[2]Gui, W. and Babuska, I., "The *h, p* and *h-p* Version of the Finite Element Method in One Dimension", Parts 1, 2 and 3, *Numerische Mathematik*, Vol. 49, pp.577-683, 1986.

[3]Oden, J. T., Wu, W. and Ainsworth, W., "Three-Step H-P Adaptive Strategy for the Incompressible Navier-Stokes Equations, Modeling, Mesh Generation, and Adaptive Numerical Methods for Partial Differential Equations", Springer-Verlag, pp. 347-366, 1995.

[4]Devloo, P., Oden, J. T. and Pattani, P., "An *h-p* Adaptive Finite Element Method for the Numerical Simulation of Compressible Flow", *Computer Methods in Applied Mechanics and Engineering*, Vol. 70, pp.203-235, 1988.

[5]Oden, J. T. and Demkowicz, L, "*h-p* Adaptive Finite Element Methods in Computational Fluid Dynamics", *Computer Methods in Applied Mechanics and Engineering*, Vol. 89, n 1-3, pp. 11-40, 1991.

[6]Oden, J. T., Kennon, S. R., Tworzydlo, W. W., Bass, J. M. and Berry, C., "Progress on Adaptive *hp*-Finite Element Methods for the Incompressible Navier-Stokes Equations", *Computational Mechanics*, Vol. 11, pp. 421-432, 1993.

[7]Chorin, A. J., "Numerical Solution of the Navier-Stokes Equations", *Mathematics of Computation*, Vol. 22, pp.745-762., 1968.

[8]Rachowicz, W., Oden, J. T. and Demkowicz, L., "Toward a Universal h-p Adaptive Finite Element Strategy, Part 3. Design of *h-p* Meshes", *Computer Methods in Applied Mechanics and Engineering,* Vol. 77, pp. 181-212, 1989.

[9]Demkowicz, L., Rachowicz, W. and Devloo, Ph., "A Fully Automatic *hp*-Adaptivity", *Journal of Scientific Computing*, Vol. 17, Nos. 1-4, December, pp. 127-155, 2002.

[10]Ainsworth, M. and Senior, B., "Aspects of an Adaptive *hp*-Finite Element Method: Adaptive Strategy, Conforming Approximation, and Efficient Solvers", *Computer Methods in Applied Mechanics and Engineering,* Vol. 150, pp.65-87, 1997.

[11]Ainsworth, M. and Senior, B., "An adaptive refinement strategy for hp-finite element computations", *Applied Numerical Mathematics,* Vol. 26, pp.165-178, 1998.

[12]De Vahl Davis, G., "Natural Convection of Air in a Square Cavity: A Bench Mark Numerical Solution", *International Journal of Numerical Methods in Fluids*, Vol. 3, 249-264, 1983.

[13]Blackwell, B. G. and Pepper, D. W., *Benchmark Problems for Heat Transfer Codes,* HTD-Vol. 222, ASME, NY, 1992.

[14]Gartling, D. K., "A Test Problem for Outflow Boundary Conditions- Flow over a Backward-Facing Step", *International Journal of Numerical Methods in Fluids*, Vol. 11, pp. 953-967, 1990.

[15]Armaly, B. F., Durst, F., Pereira, J. C. F. and Schonung, B., "Experimental and Theoretical Investigation of Backward-Facing Step Flow," *Journal of Fluid Mechanics*, Vol. 172, pp.473-496, 1983.

[16]Chen, K. S, Ku, A. C. and Chou, C. H. "Investigation of Natural Convection in Partially Divided Rectangular Enclosures Both With and Without an Opening in the Partition Plate: Measurements", *Journal of Heat Transfer*, Vol.112, pp. 648-652, 1990.